

Stereochemical and electronic interaction studies of α -heterosubstituted acetone oximes

P.R. Olivato ^{a,*}, D.S. Ribeiro ^a, R. Rittner ^b, Y. Hase ^b, D. del Pra ^c, G. Bombieri ^c

^a Instituto de Química da Universidade de São Paulo, Caixa Postal 26.077, 05599-970 São Paulo, SP, Brazil

^b Instituto de Química, Universidade Estadual de Campinas, Caixa Postal 6154, 13083-970 Campinas, SP, Brazil

^c Istituto di Chimica Farmaceutica, Viale Abruzzi 42, I-20131 Milan, Italy

Received 29 August 1994; in final form 9 January 1995

Abstract

The free $\nu_{C=N}$ bands in the IR spectra of some α -heterosubstituted acetone oximes show the existence of only a monomeric form in chloroform solutions at concentrations below 10^{-2} M, while in carbon tetrachloride self-associated species are also present. The ^1H and ^{13}C NMR chemical shift data indicate the predominance of the E over the Z isomer. The $\Delta\nu_{C=N}$ frequency shifts and molecular mechanics calculations strongly suggest that the oximes are in the gauche conformation. X-ray diffraction data have shown that the single dimethylaminoacetone oxime isomer exists in the E configuration and gauche conformation. Non-additivity effects for the α -methylene carbon chemical shifts seem to indicate the occurrence of a $\pi_{C=N}/\sigma_{C-X}^*$ interaction besides the $\pi_{C=N}^*/\sigma_{C-X}$ hyperconjugative interaction.

1. Introduction

Previous reports from this laboratory by IR, UV, NMR and UPS spectroscopies of some aliphatic α -heterosubstituted carbonyl compounds such as ketones [1,2], amides [3,4], esters [5] and thioesters [6] along with the aromatic α -heterosubstituted acetophenones [7] showed that the $\pi_{C=O}^*/\sigma_{C-X}$ hyperconjugative and the $\pi_{C=O}^*/n_X$ orbital interactions of their gauche rotamers are the main controlling factors in the cis-gauche rotational isomerism. Moreover, our studies of some α -thiosubstituted ketones and their mono- and dioxygenated derivatives [8–12] indicated the occurrence of a $\pi_{C=O}/\sigma_{C-S}^*$ orbital interaction of their gauche rotamers besides the $\pi_{C=O}^*/\sigma_{C-S}$ hyperconjugative interaction.

It should be pointed out that the $\pi_{C=Y}^*/\sigma_{C-X}$ hyperconjugative interaction for the C=Y group should increase in the series $C=C < C=N < C=O$ taking into account that the electron affinity of the π^* orbital should increase in the same order. On the contrary, the $\pi_{C=Y}/\sigma_{C-X}^*$ interaction should increase in the series $C=O < C=N < C=C$ considering that the π orbital should decrease its ionization energy in the same order. However, in the oximes [13,14], because of the mixing of $\pi_{C=N}$ and $\pi_{C=N}^*$ orbitals with the n_O oxygen lone pair of the C=N–OH group, the $\pi_{C=N}$ orbital should have a higher energy than the $\pi_{C=N}$

* Corresponding author.

orbital of the imines and even higher than the $\pi_{C=C}$ orbital. Thus, the new order of the $\pi_{C=Y}/\sigma_{C-X}^*$ interaction may be $C=O < C=N < C=C < C=N(OH)$.

In order to further investigate the nature of the electronic interactions between $\pi(\pi^*)$ and $\sigma_{C-X}(\sigma_{C-X}^*)$ orbitals, the present work describes the study of α -heterosubstituted acetone oximes, bearing as the α -substituent, representative elements from the first to the fourth rows of the Periodic Table, using IR, NMR and UV spectroscopies. Additional interest on substituted oximes arises from their easy conversion to nitroso-alkenes [15] which are useful dienophiles in Diels–Alder reactions.

It should be pointed out that there are several published papers on acetone oxime, but no study of significance has been undertaken on the heterosubstituted acetone oximes. A recent work [14] on a series of *trans*-3-alkyl-2-chloro(methoxy)cyclohexanone oximes and their derivatives by 1H NMR spectroscopy has indicated that the majority of the studied cyclohexanone oximes exist in the E configuration having a diaxial chair conformation, which suggests the occurrence of a strong $\sigma_{C-X}^* \leftarrow \pi_{C=N(OH)}$ interaction.

2. Experimental

2.1. Materials

All solvents for spectrometric measurements were spectrograde and were used without further purification. The starting materials: acetone, fluoro-, chloro-, methoxy- and dimethylamino-acetones as well as hydroxylamine hydrochloride, sulphate and phosphate were commercial products and were used without further purification. Bromo- [16] and ethylthio-acetones [17] were prepared by literature procedures. Fluoro- (1), methoxy- (2), dimethylamino- (3), chloro- (4), bromo- (5), ethylthio-acetone oximes (6) and acetone oxime (8) were obtained by an adaptation of a general literature procedure [18], i.e. by the reaction of an aqueous solution of the appropriate ketone with a slight excess of hydroxylamine sulphate, hydrochloride or phosphate followed by the addition of sodium bicarbonate portions in the molar ratio 1:1.3:1. The reaction mixture was stirred at room temperature for 2.0 h and worked up in the usual way. Iodoacetone oxime (7) was prepared by analogy to the procedure described for iodoacetone [19], i.e. by the reaction of an equimolar proportion of chloroacetone oxime and potassium iodide in dry acetone solution at room temperature (in the dark) for 2 h.

Compounds (1) and (6) are new, and although compound (2) has already been described in the literature [20,21], its physical constants have not been published. The E isomer prevails over the Z one by more than 80% for the whole heterosubstituted acetone oximes series, except for compound (3), for which only the E isomer was obtained.

The 1H NMR data of the obtained acetone oxime derivatives (1)–(8) are presented in Table 4, and their physical constants and elemental analysis are given below. Fluoro- (1) b.p. 40 °C/3.5 Torr (new compound). Analysis. Calculated for C_3H_6FNO : C, 39.56; H, 6.59; N, 15.38. Found: C, 39.59; H, 6.28; N, 14.93. Methoxy- (2) b.p. 60–62 °C/0.25 Torr. Analysis. Calculated for $C_4H_9NO_2$: C, 46.60; H, 8.74; N, 13.59. Found: C, 46.76; H, 8.72; N, 13.20. (*E*)-Dimethylamino- (3) m.p. 98–99.5 °C (Lit. [22] 97–97.5 °C). Chloro- (4) b.p. 73 °C/3.7 Torr (Lit. [22] 71.2 °C/9 Torr). Analysis. Calculated for C_3H_6ClNO : C, 33.49; H, 5.58; N, 13.02. Found: C, 33.77; H, 5.75; N, 12.80. Bromo- (5) b.p. 60 °C/0.35 Torr (Lit. [22] m.p. 36.5 °C). Analysis. Calculated for C_3H_6BrNO : C, 23.69; H, 3.95; N, 9.21. Found: C, 23.42; H, 4.19; N, 9.16. Ethylthio- (6) b.p. 74 °C/0.15 Torr (new compound). Analysis. Calculated for $C_5H_{11}NOS$: C, 45.11; H, 8.27; N, 10.53. Found: C, 45.12; H, 8.31; N, 10.59. Iodo- (7) (Lit. [22] m.p. 64.5 °C). Analysis. Calculated for C_3H_6INO : C, 18.10; H, 3.01; N, 7.04. Found: C, 18.32; H, 3.14; N, 7.20. Hydrogen- (8) m.p. 59–60 °C (Lit. [23] 65.8 °C).

2.2. Methods

The IR spectra were recorded on a Perkin-Elmer model 283 grating spectrometer at room temperature. The spectral slit width was 3.5 and 2.0 cm^{-1} in the $\nu_{\text{O-H}}$ and $\nu_{\text{C=N}}$ regions, respectively. The $\nu_{\text{O-H}}$ and $\nu_{\text{C=N}}$ frequencies were measured in the transmittance scale mode for $(3.0\text{--}5.0) \times 10^{-3} \text{ mol dm}^{-3}$ solutions in carbon tetrachloride and chloroform, using a pair of 5.0 mm potassium bromide variable path length matched cells. The $\nu_{\text{O-H}}$ bands were also measured in $1.0 \times 10^{-3} \text{ mol dm}^{-3}$ carbon tetrachloride solutions using a pair of 1.00 cm quartz matched cells.

For the weak $\nu_{\text{C=N}}$ bands a variable ordinate expansion scale in the range $2\text{--}5 \times$ was used. The spectra were calibrated with polystyrene film at 1601.4 and 2850.7 cm^{-1} . The more intense component of the $\nu_{\text{C=N}}$ band was accurate to $\pm 0.5 \text{ cm}^{-1}$ and the inflection point of the shoulder was accurate to $\pm 1 \text{ cm}^{-1}$. The free and associated $\nu_{\text{O-H}}$ bands were accurate to ± 1 and $\pm 2 \text{ cm}^{-1}$, respectively. The frequencies and intensities of $\nu_{\text{C=N}}$ and $\nu_{\text{O-H}}$ bands were measured directly at the maxima or at the inflection point (in the case of the overlapped $\nu_{\text{C=N}}$ bands).

The ^1H and ^{13}C NMR spectra of $5 \times 10^{-2} \text{ mol dm}^{-3}$ solutions in CDCl_3 , with Me_4Si as an internal reference in 5 mm o.d. sample tubes, were recorded at 200 and 50 MHz, respectively, using a Bruker AC-200 spectrometer in the FT mode. The conditions for the ^1H NMR spectra were as follows: pulse width, 7.8 μs ; acquisition time, 2.7 s; spectral width, 6024 Hz; pulse repetition time 0.0 s; number of transients, 100–200; number of data points, 32K. Similarly, for the ^{13}C NMR spectra: pulse width, 2.0 μs ; acquisition time; 1.3 s; spectral width 12 500 Hz; pulse repetition time, 1.7 s; number of transients, 20 000; number of data points, 32K. The ^{13}C NMR spectra were recorded both in the proton-noise and off-resonance decoupled modes.

The UV spectra of $10^{-4}\text{--}10^{-3} \text{ mol dm}^{-3}$ solutions in *n*-hexane and methanol using a 0.20 cm quartz cell were recorded in a Beckman DU 70 spectrometer.

2.3. Crystallography

Crystal data were collected on an Enraf Nonius CAD-4 diffractometer with graphite monochromatized Mo $\text{K}\alpha$ radiation. A white prismatic crystal ($0.15 \times 2.05 \times 0.4 \text{ mm}^3$) grown from dichloromethane solution was sealed in a capillary equilibrium with a second crystal in order to prevent its decomposition and used for data collection (the crystal easily sublimates in the air, and if coated with an epoxy polymer it decomposes). Relevant crystal data are summarized in Table 1. The structure was solved by direct methods [24] and refined by full matrix least-squares [25] with anisotropic thermal parameters for the non-hydrogen atoms. The hydrogen atoms were all found on difference Fourier maps but, except for the hydrogen of the oxygen atom refined isotropically, they were introduced at calculated positions (C–H 0.98 Å) with a unique isotropic thermal parameter ($U = 0.07 \text{ \AA}^2$). Fractional coordinates for non-hydrogen atoms are included in Table 2.

Structure factor data have been deposited with the British Library Document and Supply Centre as Supplementary Publication No. 13534 (7 pages). Retrieval information is given on the penultimate page of each issue of *Spectrochimica Acta Part A*.

2.4. Molecular mechanics calculations

The MM calculations were performed using the MM2UEC program [26] with the 1991 updated MM2(87) force field by Allinger [27] and MM2 parameters for oximes given by Schnur and Dalton [28]. The undefined parameters, X–C(sp³)–C(oxime), X–C(sp³)–C(oxime)–C(sp³) and X–C(sp³)–C(oxime)=N(oxime), were assumed to be the same as those for X–C(sp³)–C(carbonyl), X–C(sp³)–C(carbonyl)–C(sp³) and X–C(sp³)–C(carbonyl)=O, respectively, where X is the halogen atom. Numerical calculations were carried out on an IBM-PC/AT computer.

2.5. Rotamer population ratios

The rotamer population ratios were determined by the energy difference between them, using the relation

$$\Delta G^\circ = -RT \ln K$$

where the symbols have their customary meaning. For the case of the α -haloacetone oximes the equilibrium



may be determined from the fact that there are two enantiomeric gauche rotamers, one cis and one trans, for the entropy of mixing. For instance, for the (*E*)-chloroacetone oxime at 27 °C or 300 K, the cis/gauche equilibrium has $\Delta H^\circ = -0.64 \text{ kcal mol}^{-1}$ (see Table 6). Since there are two enantiomeric gauche rotamers, the free energy is related to the enthalpy change, by an entropy of mixing

$$\Delta S^\circ = R \ln 2$$

$$\Delta G^\circ = \Delta H^\circ - T\Delta S^\circ$$

$$\Delta G^\circ = -0.64 - 0.41 = -1.08 \text{ kcal mol}^{-1}$$

$$K = \frac{C_g}{C_c} = 0.176$$

Table 1
Summary of data collection and crystal parameters ^a

Formula	C ₅ H ₁₂ N ₂ O
Molecular weight	116.16
Crystal system	Monoclinic
Space group	P2 ₁ /n
Cell constants	
<i>a</i> (Å)	6.470(1)
<i>b</i> (Å)	11.801(2)
<i>c</i> (Å)	9.282(2)
β (deg)	98.09(2)
Volume: <i>V</i> (Å ³)	701.65
Molecules per cell, <i>Z</i>	4
Density (calculated), <i>D_x</i> (Mgm ⁻³)	1.10
Radiation, λ (Mo Kα) (Å)	0.71069
<i>T</i> (K)	295
Linear absorption coefficient, μ (cm ⁻¹)	0.47
Scan technique	θ/2θ
Scan width (deg)	1.2
2θ range for data collection (deg)	5.6–47.7
Number of reflections measured	1255
Number of unique reflections	886
Number of standard reflections	3
Number of observed reflections	688
<i>R</i> _i	0.013
Criterion for observed	<i>F</i> > 5σ(<i>F</i>)
<i>h</i> _{min.} , <i>h</i> _{max.} ; <i>k</i> _{min.} , <i>k</i> _{max.} ; <i>l</i> _{min.} , <i>l</i> _{max.}	–7,7; 0,12; 0,10
<i>F</i> (000)(e)	256.00
Number of parameters refined	86
Number of reflections used in refinement	688
<i>R</i> ^b	0.057
<i>R</i> _w ^c	0.059
<i>S</i>	0.544

^a Source of Atomic scattering factors: International Tables for X-Ray Crystallography, Vol. 4, 1974, Table 2.2B. ^b $R = (\sum |F_o| - |F_c|) / \sum |F_o|$. ^c $R_w = [\sum_w (|F_o| - F_c)^2 / \sum |F_o|^2]^{1/2}$; $w = 1 / [\sigma^2(F_o) + 0.022924(F_o)^2]$.

Table 2
Fractional coordinates with equivalent isotropic thermal parameters

Atom	x	y	z	U_{is} (eq.) ^a /Å ²	Bond	Distance/Å	Bond angle	Value/deg
O(1)	0.7307(3)	0.1402(2)	0.9304(2)	0.0500(8)	O(1)–N(2)	1.400(3)	O(1)–N(2)–C(5)	112.5(2)
N(2)	0.6603(4)	0.2524(2)	0.9280(2)	0.0423(8)	N(2)–C(5)	1.278(3)	C(6)–N(3)–C(8)	109.6(2)
N(3)	0.3367(3)	0.4288(2)	0.7133(2)	0.0355(8)	N(3)–C(4)	1.469(3)	C(4)–N(3)–C(8)	111.4(2)
C(4)	0.5506(4)	0.4133(2)	0.7878(3)	0.042(1)	N(3)–C(6)	1.470(4)	C(4)–N(3)–C(6)	108.8(2)
C(5)	0.6190(4)	0.2918(3)	0.7989(3)	0.0373(9)	N(3)–C(8)	1.465(4)	N(3)–C(4)–C(5)	113.6(2)
C(6)	0.2979(5)	0.5505(3)	0.6895(3)	0.052(1)	C(4)–C(5)	1.500(4)	N(2)–C(5)–C(4)	115.6(2)
C(7)	0.6421(5)	0.2283(3)	0.6638(3)	0.049(1)	C(5)–C(7)	1.484(4)	C(4)–C(5)–C(7)	119.1(2)
C(8)	0.1828(5)	0.3819(3)	0.7987(4)	0.061(1)			N(2)–C(5)–C(7)	125.2(3)

^a U equivalent is defined as one-third of the trace of the orthogonalized U_{ij} tensor.

Table 3

Frequencies (ν in cm^{-1}) and intensities (ϵ in $\text{mol}^{-1} \text{dm}^3 \text{cm}^{-1}$)^a of the O–H and C=N stretching bands in the IR spectra of α -monosubstituted acetone oximes $\text{MeC(=NOH)CH}_2\text{X}$

Compd.	X	CCl_4				CHCl_3			
		$\nu_{\text{O-H}}$	ϵ^b	$\nu_{\text{C=N}}$	10ϵ	$\nu_{\text{O-H}}$	ϵ^b	$\nu_{\text{C=N}}$	10ϵ
(1)	F	3596 ^c	142	1664	66	3575	130	1665	40
		3307 ^d	27	1672	(22) ^e				
(2)	OMe	3600	144	1662	92	3576	85	1661	90
		3304	25	1674	(18)				
(3)	NMe 2	3593	95	1661	110	3575	82	1659	60
		3286	35	1680	(19)				
(4)	Cl	3596	172	1659	75	3574	122	1657	60
		3314	14	1666	(27)				
(5)	Br	3594	170	1650	60	3575	109	1650	60
		3317	20	1655	(30)				
(6)	SEt	3597	98	1654	100	3576	155	1654	130
		3289	27	1668	(29)				
(7)	I	3593	170	1644	40	3575	135	1646	60
		3304	24	1649	(26)				
(8)	H	3603	157	1665	135	3580	67	1665	130
		3299	31	1677	(45)				

^a ϵ is the apparent molar absorptivity. ^b Estimated directly at the absorption maximum ($\nu_{\text{O-H}}$, $\nu_{\text{C=N}}$) or at the inflection point ($\nu_{\text{C=N}}$) of the overlapped bands. ^{c,d} Free and associated $\nu_{\text{O-H}}$ bands. ^e Shoulder.

3. Results and discussion

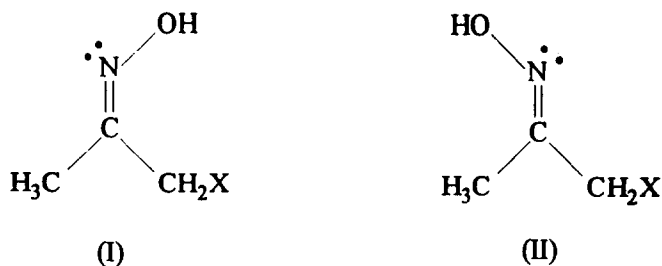
3.1. $\nu_{\text{O-H}}$ and $\nu_{\text{C=N}}$ stretching bands

Table 3 shows the $\nu_{\text{O-H}}$ and $\nu_{\text{C=N}}$ stretching frequencies and intensities of some α -heterosubstituted acetone oximes (1)–(7) in carbon tetrachloride and chloroform. Corresponding data for the parent acetone oxime (8) are included.

Inspection of Table 3 shows that the oximes in carbon tetrachloride in the range of concentration $(3-5) \times 10^{-3} \text{ M}$ display a sharp $\nu_{\text{O-H}}$ band at about 3600 cm^{-1} which corresponds to the monomer, followed by a weak associated band near 3300 cm^{-1} (Fig. 1(a)). On the contrary, the oximes in the polar solvent chloroform, at the same concentration of carbon tetrachloride, show only the $\nu_{\text{O-H}}$ free band near 3575 cm^{-1} .

It should be pointed out that the $\nu_{\text{C=N}}$ band follows the same pattern as the $\nu_{\text{O-H}}$ band, i.e. in carbon tetrachloride solution a weak shoulder at the higher frequency side of the main $\nu_{\text{C=N}}$ band may be observed (Fig. 1(c)), while it is absent in chloroform.

Concentration effects on the associated $\nu_{\text{O-H}}$ and $\nu_{\text{C=N}}$ bands are shown in Fig. 1. The disappearance of the associated $\nu_{\text{O-H}}$ band in a $1 \times 10^{-3} \text{ mol dm}^{-3}$ solution for the whole oxime series (1)–(7) precludes the existence of any intramolecular hydrogen bonding between the OH proton and the α -heteroatom in the Z isomer (Structure I). It is well known [29,30] that the self-association of the oximes in the gas phase and in solution, through hydrogen bonding between the OH group and the nitrogen lone pair of the azomethyne group (C=N-OH), originates dimers and trimers which shift the equilibrium towards the monomer with progressive dilution.



Structures I and II.

The $\nu_{\text{O-H}}$ free band frequency shift from a carbon tetrachloride to a chloroform solution (about 20 cm^{-1} , see Table 3) for the whole series may be ascribed to the dipole-dipole interaction between the acidic OH group and the chloroform polar molecules.

The $\nu_{\text{C=N}}$ shifts to higher frequencies due to self-association in carbon tetrachloride solution are similar to the shifts for nitriles in the presence of a proton donor [31–33].

On the contrary, no $\nu_{\text{C=N}}$ frequency shifts are observed on going from a carbon tetrachloride to a chloroform solution. The azomethyne group of the oximes should be less polar than the same group of the imines taking into account that besides the

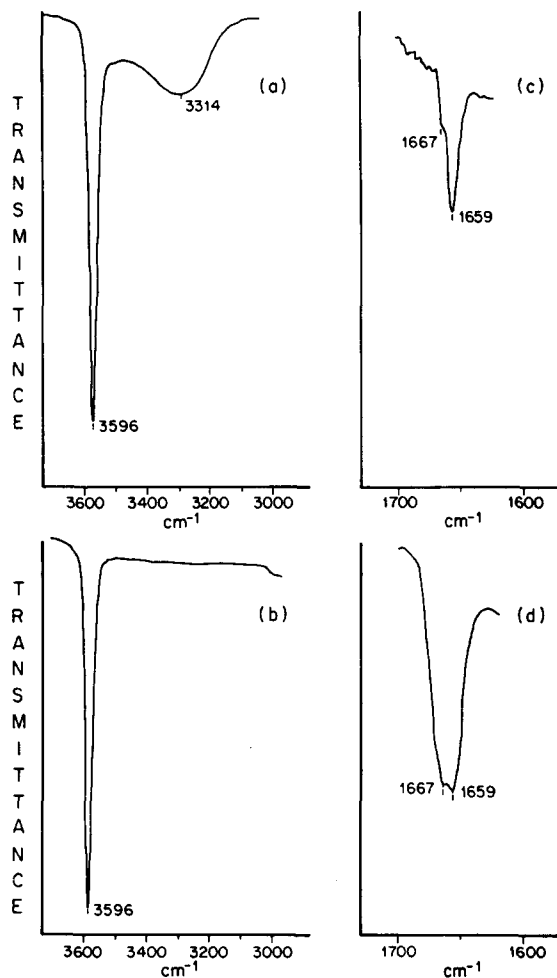


Fig. 1. Free and associated $\nu_{\text{O-H}}$ and $\nu_{\text{C=N}}$ IR bands of chloroacetone oxime (4), in carbon tetrachloride, showing: (i) the disappearance of the $\nu_{\text{O-H}}$ associated band on going from (a) $C = 5.0 \times 10^{-3}$ to (b) $C = 1.0 \times 10^{-3}\text{ mol dm}^{-3}$ solutions; (ii) the increasing of the associated band in relation to the free band on going from (c) $C = 5.0 \times 10^{-3}\text{ mol dm}^{-3}$ to (d) $C = 0.1\text{ mol dm}^{-3}$ solutions.

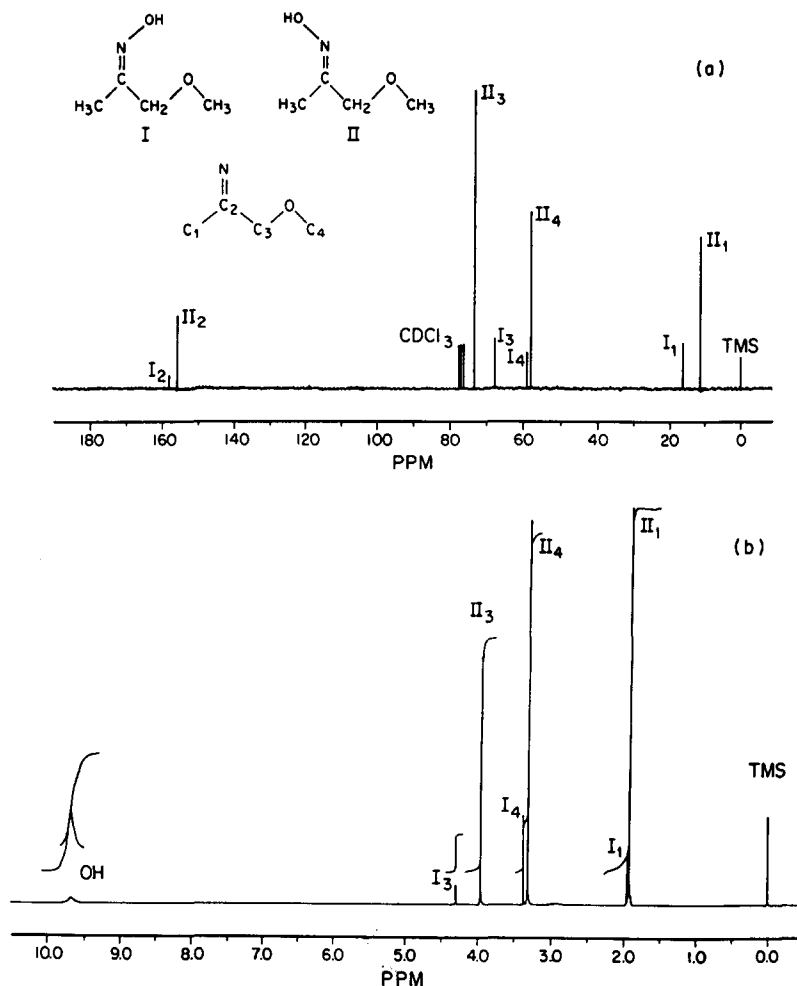


Fig. 2. ¹³C (a) and ¹H (b) NMR spectra of methoxyacetone oxime (2) isomers in CDCl₃ showing the predominance of the E over the Z diastereomer.

[>C[⊕]-N[⊖]] resonance structure for the oximes there is also the contribution of the [>C=N-OH] structure [14] which decreases in part the normal $\delta^+C=N\delta^-$ polarization and increases the acidity of the OH proton. Thus, some decreasing of the $\nu_{C=N}$ frequency should be expected in the polar solvent chloroform, but this effect is practically cancelled out due to the hydrogen bonding between the chloroform proton and the oxime nitrogen lone pair, which would cause the $\nu_{C=N}$ frequency to increase slightly.

3.2. ¹³C and ¹H NMR chemical shifts

Table 4 shows the experimental proton and carbon chemical shifts of the α -heterosubstituted acetone oximes (1)–(7) and of the parent compound (8), as well as the calculated α -methylene carbon chemical shifts.

The ¹H NMR chemical shifts were assigned through the well-known chemical shift rules [34], from their relative intensities (see Fig. 2(b)), and from a 2D carbon–proton experiment (see below). It is noteworthy that the α -methylene protons display an inverse behaviour in comparison with the corresponding carbon chemical shifts, i.e. for the Z isomer the α -methylene proton signal is downfield while the methylene carbon signal is upfield in relation to the same nuclei of the E isomer.

The ¹H and ¹³C NMR spectra of most of the studied oximes (compounds (1), (2) and (4)–(7)) show a large predominance of one diastereomer (>80% as shown in Table 4; estimated from their proton spectra; see Fig. 2(b)), which was ascribed to the E isomer

Table 4
 ^1H and ^{13}C NMR chemical shifts (δ)^a of α -heterosubstituted acetone oximes $\text{MeC(=NOH)CH}_2\text{X}$ in CDCl_3

Compd.	X	Config. ^b	CH_3 ^c	CH_3	OH^d	C(=NOH)	CH_2	CH_2	CH_2	Nucleus of X substituent			Z/E ^d	
										$\alpha\text{-CH}_2$	$\alpha\text{-CH}_2$	$\beta\text{-CH}_3$		$\beta\text{-CH}_3$
(1)	F	Z	1.98	15.16 ^f	9.61	157.05 ^f	5.28 ^g	78.64 ^f (85.1) ^h					25	
		E	1.99	11.00		154.39 ^f	4.86 ^g	83.06 ^f (92.2)						
(2)	OMe	Z	1.95	16.21	9.68	157.87	4.31	67.66 (74.1)	3.38	58.97				17
		E	1.94	11.28		155.71	3.86	73.41 (81.2)	3.32	57.86				
(3)	NMe_2	E	1.95	12.35	10.18	156.00	2.98	63.54 (68.2)	2.27	45.22			0	
(4)	Cl	Z	1.97	18.02	9.33	154.62	4.22	36.25 (46.1)					13	
(5)	Br	E	1.95	12.37		154.62	4.02	45.46 (53.2)						
		Z	2.05	18.52	9.23	153.43	4.09	21.11 (34.6)					17	
(6)	SEt	E	2.04	12.52		154.71	3.97	32.64 (41.7)						
		Z	2.04	18.60	9.68	155.68	3.42	26.98 (33.2)	2.54 ⁱ	26.04	1.27 ⁱ	14.57	20	
(7)	I	E	2.00	12.59		155.68	3.21	35.87 (40.3)	2.46 ⁱ	25.0	1.23 ⁱ	14.29		
		Z	–	18.39	9.10	154.35	4.07	–8.2 (4.1)					10	
(8)	H	E	2.04	13.20		155.49	3.87	5.1 (11.2)						
		–	1.88	21.66 ^j	8.50	155.7								
			1.89	14.6										

^a In ppm relative to Me_4Si . ^b Z and E refer to NOH syn and anti to the CH_2X group, respectively. ^c Refers to the more intense peak of the unresolved doublet. ^d Averaged OH proton shifts for both isomers. ^e Ratio of isomers (%) from the corresponding integrated intensities of the methylene proton signal from the ^1H NMR spectra. ^f Mean chemical shift values of the doublets due to carbon-fluorine coupling $J_{\text{C-F}}$ whose constants in Hz are: ¹ $J = 9.7$, ² $J = 23.1$, ³ $J = 17.9$, ⁴ $J = 166.7$, ⁵ $J = 166.0$, respectively. ^g Mean chemical shift values of doublets due to proton-fluorine coupling whose constant is ² $J_{\text{HF}} = 12.0$ Hz. ^h Calculated values (see text). ⁱ ³ $J = 7.40$ Hz. ^j Methyl carbon anti to the OH group, assigned according to Ref. [35].

(Structure II) from NOE-differential experiments (compound (3), positive enhancement for the methyl protons signal followed by a negative NOE for the dimethylamino protons on irradiation of the OH proton) and from a 2D carbon–proton correlated spectrum (compound (4)), the latter to confirm the correspondence of the more intense signals both in the ^1H and ^{13}C NMR spectra (see Fig. 2). The observed upfield shift due to the steric compression between the methyl carbon syn to the OH group (as well as for the methylene carbon) has been described previously by Levy and Nelson [35] for the methylethylketone oxime.

The agreement in the methyl carbon chemical shifts values (compounds (1)–(7), $\delta(\text{CH}_3)$ 11.0–13.20; compound (3), $\delta(\text{CH}_3)$ 12.35) and with a previous literature description for compound (3) configuration [36] corroborate our assignments. Furthermore, X-ray diffraction data confirm the E configuration for the compound (see below).

Empirical calculations of the α -methylene carbon chemical shifts, according to a Grant–Paul related method [37,38], have also confirmed the above assignments (Table 4), despite the non-additivity effects ($\Delta\delta = \delta_{\text{exp.}} - \delta_{\text{calc.}}$), which are shown in Table 5 are thoroughly discussed in the next section.

3.3. C=N stretching frequency shifts and non-additivity effects of α -methylene carbon chemical shifts

Table 5 shows the frequency shifts ($\Delta\nu$) of the single weak $\nu_{\text{C=N}}$ band of the α -heterosubstituted acetone oximes in chloroform, along with the computed carbonyl frequency shifts [1] induced by the α -substituents' hyperconjugative effect ($\Delta\nu_{\text{H}}$) for the corresponding monosubstituted acetones. The estimation of the carbonyl frequency shifts induced by the hyperconjugative effect ($\Delta\nu_{\text{H}}$) from the $\Delta\nu_{\text{g}}$ values ($\Delta\nu_{\text{g}} = \Delta\nu_{\text{H}} + \Delta\nu_{\text{I}}$; $\Delta\nu_{\text{I}}$ corresponding to the inductive contribution) has been described fully in a previous paper [1].

The observed C=N frequency shifts are all negative and vary from 0 to -19 cm^{-1} for the whole series (1)–(7) and are quite close to the $\Delta\nu_{\text{H}}$ values which vary from 0 to -16 cm^{-1} (Table 5). Both frequency shifts are well correlated ($r = 0.987$; $s = 1.27\text{ cm}^{-1}$). The sulphur derivative (6) was excluded, because it deviates slightly from the correlation ($r = 0.916$; $s = 2.4\text{ cm}^{-1}$).

The quite good correlation obtained between $\Delta\nu_{\text{H}}$ and $\Delta\nu_{\text{C=N}}$ frequency shifts of the E isomers of the corresponding α -heterosubstituted acetone oximes (1)–(7) strongly suggests that the oximes should have similar geometries to the corresponding acetones, i.e. gauche for the whole series, except for the fluoro derivative (1) which should be trans.

Aiming to compare the geometries of the E and Z isomers of the α -heterosubstituted acetone oximes with those of the corresponding α -heterosubstituted acetones, MM calculations were performed for the acetone oximes bearing in the α -position simple

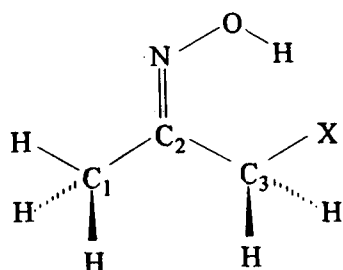
Table 5

Azomethyne (C=N) frequency shifts ($\Delta\nu$) for the E isomer gauche rotamer and non-additivity effects (NAE) for the α -methylene carbon chemical shift ($\Delta\delta_{\text{CH}_2}$) in α -monosubstituted oximes $\text{MeC(=NOH)CH}_2\text{X}$: computed carbonyl frequency shifts induced by the substituents' hyperconjugative effect ($\Delta\nu_{\text{H}}$) and corresponding NAE, in α -monosubstituted acetones

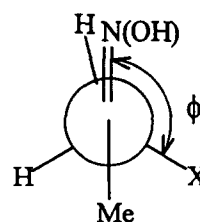
Compd.	X	$\Delta\nu_{\text{C=N}}^{\text{a}}$	$\Delta\nu_{\text{H}}^{\text{b}}$	$\Delta\delta_{\text{CH}_2(\text{Z})}^{\text{c}}$	$\Delta\delta_{\text{CH}_2(\text{E})}^{\text{c}}$	$\Delta\delta_{\text{CH}_2}^{\text{d}}$
(1)	F	0	0	-6.46	09.14	-13.7
(2)	OMe	-4	-2.1	-6.44	-7.79	-9.8
(3)	NMe ₂	-6	-4.2	-	-4.66	-5.1
(4)	Cl	-8	-8.1	-9.65	-7.74	-11.6
(5)	Br	-15	-11.6	-13.49	-9.06	-13.9
(6)	SEt	-11	-15.5	-6.22	-4.43	-5.8
(7)	I	-19	-16.2	-12.3	-5.90	-11.6

^a In cm^{-1} , for CHCl_3 solutions; $\Delta\nu_{\text{C=N}}$ refers to the difference: $\nu_{(\text{E-substituted acetone oxime})} - \nu_{(\text{acetone oxime})}$ for the gauche rotamers (see text). ^b In cm^{-1} , taken from Ref. [1]. ^c $\Delta\delta = \delta_{\text{exp.}} - \delta_{\text{calc.}}$ (data from Table 2). ^d From Ref. [38].

substituents such as the halogen atoms F, Cl, Br and I. Table 6 shows that for the Z isomers of the title compounds there is only one minimum of energy for the Cl (4), Br (5) and I (6) derivatives which corresponds to the gauche (or trans) conformations ($96^\circ < \phi < 180^\circ$) (Structure IV). The F (1) derivative presents two energy minima which correspond to the cis ($\phi = 0^\circ$) and trans ($\phi = 180^\circ$) conformers. On the contrary, the E isomers display two energy minima for the whole series, which correspond to the cis and gauche (or trans for F (1)) conformers.



(III)



(IV)

Structures III and IV.

It is noteworthy that the gauche (or trans) rotamers for the Z isomers ((4), (5) and (7)) are more stable than the corresponding rotamers of the E isomers by 0.1 to 1.0 kcal mol⁻¹ (see Table 6), except for the case of the cis conformer of the E isomer of the fluoro derivative (1), which is more stable than the cis rotamer of the Z isomer by 1.5 kcal mol⁻¹. The apparent disagreement between the MM data (thermodynamic preference for the Z isomer) and our experimental results is attributed to the method of preparation of the oximes employed here.

Moreover, there is a remarkable parallelism between the geometries of the α -haloacetone oximes and those of the corresponding acetones. Both the Z and E isomers of the fluoroacetone oxime (1) present a trans geometry, and the chloro- (4), bromo- (5) and iodoacetone oximes (7) show gauche (or trans) geometries, whose dihedral angles are very close to the ones previously estimated for the α -haloacetones [7] through MM calculations.

The MM data (Table 6) are of paramount importance because they support the $\Delta\nu_{C=N}$ frequency shift analysis, indicating that the acetone oximes obtained, which are to a large extent (> 80%) in the E configuration, present a gauche conformation for the Cl, Br and I substituents and a trans conformation for the F substituent. Moreover, the X-ray diffraction data for the dimethylaminoacetone oxime showed that it exists in the solid state in the gauche conformation (see below).

It should be pointed out that while the inductive contribution $\Delta\nu_I$ to $\Delta\nu_g$ (see Ref. [1] for the carbonyl frequency shifts of the α -heterosubstituted acetones) is significant, the similarity between the $\Delta\nu_H$ and $\Delta\nu_g$ values for the azomethine stretching frequencies of the α -heterosubstituted acetone oximes (Table 5) indicate that the $\Delta\nu_I$ values are negligible for this series.

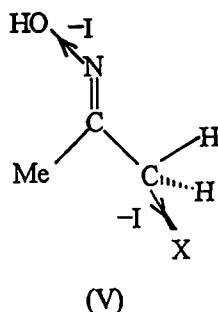
The lack of a net inductive effect for the oximes may be the result of the low polarity of the =N–OH group, together with a competition between the σ_I (0.27) value for the OH attached to the azomethine group and the substituent inductive effect, which vary from 0.47 (F) to 0.05 (NMe₂) (Structure V).

It should be mentioned that it was not possible to detect the $\nu_{C=N}$ band both for the E series cis isomers as for the Z series cis and trans (or gauche) conformers, predicted by the MM calculations (Table 6), due to the low intensity of the $\nu_{C=N}$ band and to the low proportion of the Z diastereomer (< 20%).

Table 6
 Calculated molecular mechanics energies, electric dipole moments, dihedral angles^a for the minimum energy configurations and conformations, and the relative rotamer populations for the Z- and E- α -haloacetone oximes MeC(=NOH)CH₂X

Compd.	X	$\angle \text{ONC}_2\text{C}_3 = 0^\circ (\text{Z})^b$					$\angle \text{ONC}_2\text{C}_3 = 180^\circ (\text{E})^b$					
		Conf. ^c	$\angle \text{NC}_2\text{C}_3\text{X}/\text{deg}$	μ/D	$E/\text{kcal mol}^{-1}$	$\Delta E/\text{kcal mol}^{-1}$	$c/g(\text{t})^d$	Conf. ^c	$\angle \text{NC}_2\text{C}_3\text{X}/\text{deg}$	μ/D	$E/\text{kcal mol}^{-1}$	$\Delta E/\text{kcal mol}^{-1}$
(1)	F	c	0	2.670	4.79	3.63	0.01	c	0	2.478	1.03	0.18
		t	180	0.828	1.16	0 ^e	0	t	180	0.900	0	0.18
(4)	Cl	f	–	–	–	–	0	c	0	2.534	0.64	0.18
		t	180	0.968	1.87	–	0	g	140	1.241	0	0.02
(5)	Br	f	–	–	–	–	0	c	0	2.395	1.85	0.02
		g	105	1.608	1.52	–	0	g	114	1.480	0	0.02
(7)	I	f	–	–	–	–	0	c	0	1.950	2.04	0.02
		g	96.5	1.361	0.32	–	–	g	96.5	1.269	0	0.02

^a Dihedral angles in relation to the reference structure III, where $\angle \text{HONC}_2 = 0^\circ$, $\angle \text{ONC}_2\text{C}_3 = 0^\circ$ and $\angle \text{NC}_2\text{C}_3\text{X} = 0^\circ$. ^b $\angle \text{HONC}$ dihedral angle for both Z and E configurations is 180° . ^c c, g and t refer to the cis, gauche and trans conformations, respectively. ^d Relative rotamer populations. ^e Zero energy corresponds to the minimum energy conformation. ^f There is no minimum of energy which corresponds to the cis conformation (see text for details).



Structure V.

The α -methylene carbon chemical shift non-additivity effects (NAE) [39] for the α -heterosubstituted acetone oxime E isomers ($\Delta\delta_{\text{CH}_2(\text{E})}$; Table 5) are well correlated with the corresponding $\Delta\delta_{\text{CH}_2}$ values for the α -heterosubstituted acetones ($r = 0.979$; $s = 0.39$ ppm; the iodo derivative (7) was excluded because it deviates from the correlation).

The observed correlation strongly corroborates the IR C=N frequency shift analysis, which has indicated the existence of a single gauche conformer for the E diastereomers of the title compounds, except for the fluorine derivative which seems to exist in the trans conformation. It also suggests that the electronic interactions which take place between C=N and C-X groups in the gauche conformers of the E heterosubstituted acetone oximes should be similar to those which occur between C=O and C-X groups in the gauche rotamers of the heterosubstituted acetone series.

According to Nesmeyanov et al. [40] additional shielding on the α -methylene carbon may be ascribed to an increase in the double bond character between the α -methylene and the carbonyl carbons due to the $\pi_{\text{C=O}}^*/\sigma_{\text{C-X}}$ hyperconjugation. This explanation should also be valid for the heterosubstituted acetone oximes where $\pi_{\text{C=N}}^*/\sigma_{\text{C-X}}$ hyperconjugative interaction takes place.

The NAE in the chemical shifts for the E isomers of the heterosubstituted acetone oximes are smaller than those of the corresponding heterosubstituted acetones, and they indicate [8–12] that besides the $\pi_{\text{C=N}}^*/\sigma_{\text{C-X}}$ hyperconjugation, a $\pi_{\text{C=N}}/\sigma_{\text{C-X}}^*$ interaction is also operating.

This proposition is supported by the closer proximity of the empty unperturbed $\sigma_{\text{C-X}}^*$ orbitals to the unperturbed $\pi_{\text{C=N(OH)}}$ orbital energy level (IE 9.67 eV for $\text{Me}_2\text{C=N(OH)}$ [13]) in relation to the unperturbed $\pi_{\text{C=O}}$ orbital energy level (IE 13.4 eV for $\text{Me}_2\text{C=O}$ [41]). According to the molecular orbital simple perturbation theory [42] it may be easily concluded that the $\pi_{\text{C=N}}/\sigma_{\text{C-X}}^*$ orbital interaction (δE_2 ; $\delta E = E(\text{perturbed}) - E(\text{unperturbed})$) should occur to a larger extent in the oxime series than the $\pi_{\text{C=O}}/\sigma_{\text{C-X}}^*$ orbital interaction (δE_1) in the acetone series. However, the unperturbed $\sigma_{\text{C-X}}$ orbitals [43–45] are closer to the perturbed $\pi_{\text{C=O}}^*$ orbital energy level (AE 1.31 eV for $\text{Me}_2\text{C=O}$ [46]) than to the unperturbed $\pi_{\text{C=N(OH)}}^*$ orbital energy level (AE 2.2 eV for $\text{Me}_2\text{C=N(OH)}$ [47]). Thus, it may also be concluded that the $\pi_{\text{C=O}}^*/\sigma_{\text{C-X}}$ hyperconjugative interaction (δE_1) will occur to a larger extent in the acetone series than the $\pi_{\text{C=N}}^*/\sigma_{\text{C-X}}$ hyperconjugative interaction (δE_2) in the oxime series.

The electron affinity of the $\sigma_{\text{C-X}}^*$ unperturbed orbital increases progressively on going from fluoro- (9.87 eV) to iodomethane (1.44 eV) [48,49]. Hence, it is evident that a stronger $\pi_{\text{C=N}}/\sigma_{\text{C-X}}^*$ (or $\pi_{\text{C=O}}/\sigma_{\text{C-X}}^*$) orbital interaction should occur with the $\sigma_{\text{C-I}}^*$ orbital and a weaker one with the $\sigma_{\text{C-F}}^*$. The unperturbed $\sigma_{\text{C-X}}$ orbital ionization energy [43–45] decreases in the same direction, i.e. from fluoro- to iodomethane, and therefore a stronger $\pi_{\text{C=N}}^*/\sigma_{\text{C-X}}$ ($\pi_{\text{C=O}}^*/\sigma_{\text{C-X}}$) interaction should occur with the $\sigma_{\text{C-I}}$ orbital and a weaker one with the $\sigma_{\text{C-F}}$ orbital. Therefore, it may be inferred that for the oxime and for the acetone series both orbital interactions increase in the same direction.

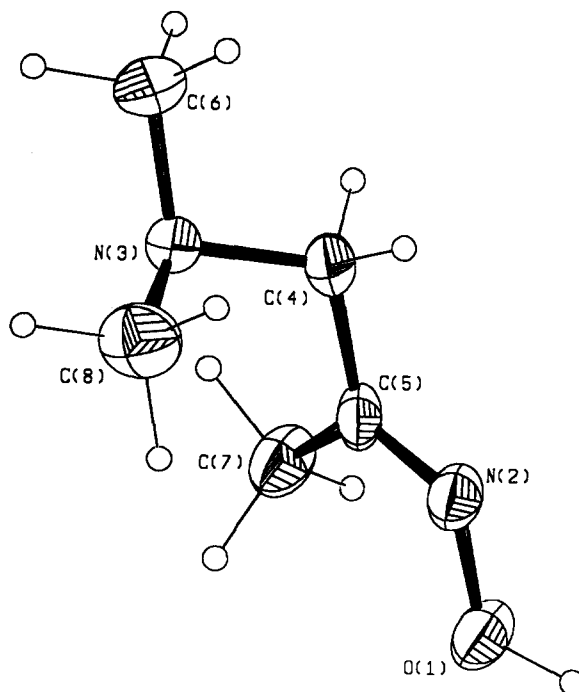


Fig. 3. ORTEP view (with thermal ellipsoids) at the 40% probability level of the molecular structure for the dimethylaminoacetone oxime (3) showing the atom numbering.

Moreover, both $\pi_{\text{C}=\text{N}}^*/\sigma_{\text{C}-\text{X}}$ (or $\pi_{\text{C}=\text{O}}^*/\sigma_{\text{C}-\text{X}}$) and $\pi_{\text{C}=\text{N}}/\sigma_{\text{C}=\text{N}}^*$ (or $\pi_{\text{C}=\text{O}}/\sigma_{\text{C}=\text{O}}^*$) orbital interactions lead to a decrease in the C=N or C=O bond order and consequently in their frequencies. These interactions act in the same direction in relation to the $\Delta\nu_{\text{H}}$ parameters, irrespective of which is the predominant one, and this gives support to our assumption of $\Delta\nu_{\text{H}}$ values quasi-equality for both oxime and acetone series.

3.4. Dimethylaminoacetone oxime X-ray analysis

An ORTEP view of a single molecule of (3) is shown in Fig. 3. The molecular structure is characterized by the N(3)–C(4)–C(5)–N(2) torsion angle of $-116.8(3)^\circ$ and by a planar C(7)–C(5)–N(2)–O(1) residue (torsion angle $-0.0(4)^\circ$). Bond distances and angles (Table 2) are in the range of observed values for similar oxime derivatives [50–52].

Intermolecular interactions essentially involve van der Waals forces and a strong hydrogen bond between the hydrogen atom at the oxime oxygen O(1) as a donor and the N(3) atom as an acceptor. The intermolecular separation O(1)–N(3) is $2.743(3) \text{ \AA}$, while H(1)–N(3) is $1.73(4) \text{ \AA}$ with an angle O(1)–H(1)–N(3) of $169(3)^\circ$. The angles around N(3) are all about 109° indicating an evident pyramidalization of the bonds which favours the interaction of the lone pair with the oxime adjacent hydrogen. The hydrogen bonding scheme illustrated in Fig. 4 determines the formation of infinite chains developing normally to the *b* axis direction.

3.5. Azomethyne (C=N) $\pi \rightarrow \pi^*$ and $n_{\text{N}} \rightarrow \pi^*$ transition energies and intensities

Table 7 shows the $\pi \rightarrow \pi^*$ and $n_{\text{N}} \rightarrow \pi^*$ transition energies and their intensities for compounds (1)–(8) in *n*-hexane and methanol.

By analogy to the assignments of the UV gas-phase spectra of some simple oximes like acetoxime [13], the $n \rightarrow \pi^*$ band of the title compounds (in *n*-hexane) appears in the range 208–218 nm as a shoulder of the more intense $\pi \rightarrow \pi^*$ band (193–199 nm), except

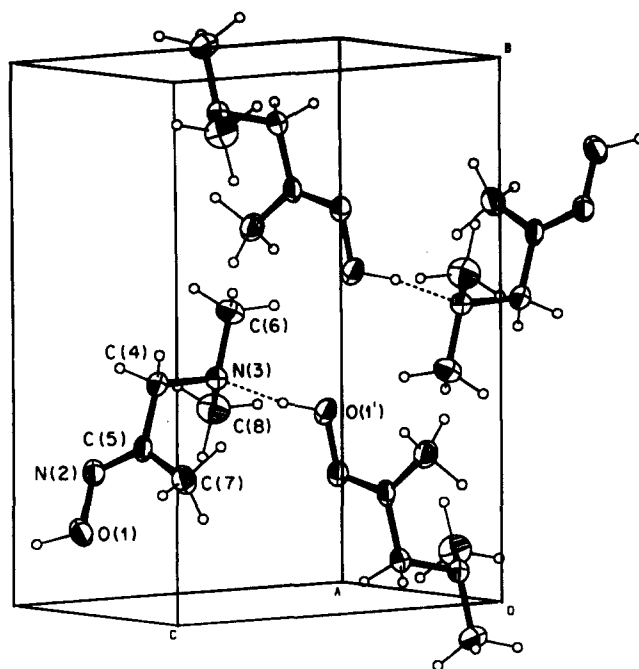


Fig. 4. Unit cell content for compound (3) (dashed lines indicate hydrogen bond interactions).

for the chloro- (4) and bromo- (5) derivatives, for which the $n \rightarrow \pi^*$ band is hidden by the $\pi \rightarrow \pi^*$ band.

The $n_{\text{N}} \rightarrow \pi^*$ band exhibits a blue shift and vanishes, in methanol, under the more intense and bathochromically shifted $\pi \rightarrow \pi^*$ band, which appears in the range 198–203 nm. It should be pointed out that while there is not a clear trend for the $\pi \rightarrow \pi^*$ band, on going from the fluoro- (1) to the iodoacetone oxime (7), the $n_{\text{N}} \rightarrow \pi^*$ band presents a slight bathochromic shift of 7 nm from the fluoro- (1) to the iodo- (7) derivative, i.e. from 211 to 218 nm. This shift is smaller than that observed previously for the corresponding heterosubstituted acetones [1] (about 26 nm). The smaller bathochromic shift of the heterosubstituted acetone oxime series (1)–(7) is further evidence of the occurrence of the $\pi_{\text{C=N}}/\sigma_{\text{C-X}}^*$ orbital interaction in these compounds.

Table 7

UV data (λ/nm) for the $\pi \rightarrow \pi^*$ and $n_{\text{N}} \rightarrow \pi^*$ transitions of the α -monosubstituted acetone oximes (1)–(8)

Compd.	X	<i>n</i> - C ₆ H ₁₄		MeOH	
		λ	$\log \epsilon^{\text{a}}$	λ	$\log \epsilon^{\text{a}}$
(1)	F	194 ^b	3.58	200	3.57
		211 ^c	2.94	–	–
(2)	OMe	196	3.65	199	3.66
		212	2.78	–	–
(3)	NMe ₂	194	3.62	199	3.68
		212	3.18	–	–
(4)	Cl	195	3.79	201	3.82
(5)	Br	199	3.60	203	3.72
(6)	SEt	194	3.92	201	3.87
		218	3.45	–	–
(7)	I	194	3.82	198	3.91
		218	3.59	224 ^d	3.82
(8)	H	193	3.48	199	3.47
		208	2.96	–	–

^a ϵ is the apparent molar absorptivity in $\text{dm}^3 \text{mol}^{-1} \text{cm}^{-1}$. ^b $\pi \rightarrow \pi^*$ transition. ^c $n_{\text{N}} \rightarrow \pi^*$ transition (a shoulder of the $\pi \rightarrow \pi^*$ absorption band). ^d Shoulder.

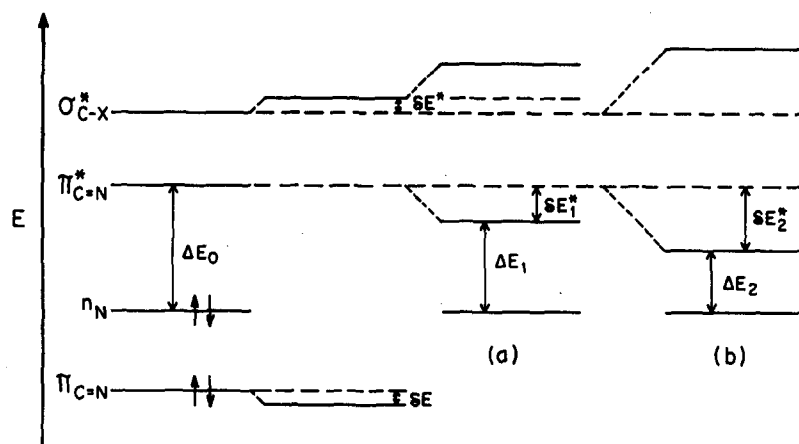


Fig. 5. Qualitative energy level diagram of the $\pi_{C=N}$, n_N , $\pi_{C=N}^*$ and σ_{C-X}^* orbitals for the gauche rotamer of the E-heterosubstituted oximes, showing the hyperconjugative interaction between the $\pi_{C=N}^*$ and σ_{C-X}^* orbitals before (b) and after (a) $\sigma_{C-X}^*/\pi_{C=N}^*$ orbital interaction, and the origin of the hypsochromic $n \rightarrow \pi^*$ shift (ΔE_1) for (a) in relation to ΔE_2 for (b).

In fact, due to the $\sigma_{C-X}^*/\pi_{C=N}^*$ hyperconjugative interaction in the excited state, a stabilization of the unperturbed $\pi_{C=N}^*$ orbital energy level by δE_2^* (Fig. 5(b)) should be expected, leading to a bathochromic shift (ΔE_2) of the $n_N \rightarrow \pi^*$ transition in relation to the transition from the n_N to the unperturbed $\pi_{C=N}^*$ orbital energy level of the acetone oxime (ΔE_0) [48] (ΔE_0). As the unperturbed σ_{C-X}^* orbital energy level of the heterosubstituted methane [48,49,53,54] becomes closer to the unperturbed $\pi_{C=N}^*$ energy level on going from the fluoro to the iodo substituent, a stronger orbital interaction should occur in this direction, leading to a progressive bathochromic shift of the $n_N \rightarrow \pi^*$ transition. However, the relative proximity of the σ_{C-X}^* and $\pi_{C=N}$ (IE 9.67 eV for $\text{Me}_2\text{C}=\text{NOH}$ [13]) unperturbed orbital energy levels pushes the σ_{C-X}^* orbital level up by δE^* leading to a decrease in the $\pi_{C=N}^*/\sigma_{C-X}^*$ hyperconjugative interaction (δE_1^*) and consequently to a larger $n_N \rightarrow \pi^*$ energy gap (ΔE_1) (Fig. 5(a)). This behaviour should originate a smaller bathochromic shift of the $n_N \rightarrow \pi^*$ transition for the oximes in relation to the corresponding acetones, on going from the fluoro to the iodo substituent, once the $\pi_{C=N}/\sigma_{C-X}^*$ interaction is stronger than the $\pi_{C=O}/\sigma_{C-X}^*$ interaction. In fact, the σ_{C-X}^* orbital is far away from the heterosubstituted acetones unperturbed $\pi_{C=O}$ energy level (IE 13.4 eV for acetone) [41] in relation to the $\pi_{C=N}$ orbital for the corresponding oximes.

Acknowledgements

The authors thank the Fundação de Amparo à Pesquisa do Estado de São Paulo and PADCT for financial support of this research and the Conselho Nacional de Desenvolvimento Científico e Tecnológico for a scholarship (to D.S.R.) and for a grant (to P.R.O. and R.R.).

References

- [1] S.A. Guerrero, J.R.T. Barros, B. Wladislaw, R. Rittner and P.R. Olivato, *J. Chem. Soc., Perkin Trans. 2* (1983) 1053.
- [2] P.R. Olivato, S.A. Guerrero, A. Modelli, G. Granozzi, D. Jones and G. Distefano, *J. Chem. Soc., Perkin Trans. 2* (1984) 1505.
- [3] M.A.P. Martins, R. Rittner and P.R. Olivato, *Spectrosc. Lett.*, 14 (1981) 505.
- [4] D. Klapstein, P.R. Olivato, F. Oike, M.A.P. Martins and R. Rittner, *Can. J. Spectrosc.*, 33 (1988) 161.
- [5] P.R. Olivato, D. Klapstein, R. Rittner, E.L. Silva and J.C.D. Lopes, *Can. J. Appl. Spectrosc.*, 37 (1992) 37.

- [6] P.R. Olivato, R. Nanartonis and J.C.D. Lopes, *Phosphorus, Sulfur, Silicon Relat. Elem.*, 71 (1992) 107.
- [7] P.R. Olivato, S.A. Guerrero, Y. Hase and R. Rittner, *J. Chem. Soc., Perkin Trans. 2* (1990) 465.
- [8] P.R. Olivato, B. Wladislaw and S.A. Guerrero, *Phosphorus, Sulfur*, 33 (1987) 135.
- [9] E. Bonfada, M.Sc. Thesis, University of São Paulo, 1989.
- [10] M.G. Mondino, M.Sc. Thesis, University of São Paulo, 1989.
- [11] P.R. Olivato and M.G. Mondino, *Phosphorus, Sulfur, Silicon Relat. Elem.*, 59 (1991) 219.
- [12] G. Distefano, M.G. Dal Colle, V. Bertolasi, R. Olivato, E. Bonfada and M.G. Mondino, *J. Chem. Soc., Perkin Trans., 2* (1991) 1195.
- [13] A. Dargelos and C. Sandorfy, *J. Chem. Phys.*, 67 (1977) 3011.
- [14] S.E. Denmark, M.S. Dappen, N.L. Sear and R.T. Jacobs, *J. Am. Chem. Soc.*, 112 (1990) 3466.
- [15] T.L. Gilchrist, *Chem. Soc. Rev.*, 12 (1993) 53.
- [16] P.A. Levene, *Org. Synth.*, 2 (1943) 88.
- [17] G. Bergson and A.L. Delin, *Ark. Kemi*, 18 (1962) 489.
- [18] P.A.S. Smith, *The Chemistry of Open-Chain Organic Nitrogen Compounds*, Vol. 2, W.A. Benjamin, New York, 1966, p. 63.
- [19] H. Lumbroso, Ch. Liegois, S.A. Guerrero, P.R. Olivato and Y. Hase, *J. Mol. Struct.*, 162 (1987) 141.
- [20] P. Plath, K. Eicken, B. Zeeh, V. Eichenauer, H. Hagen, R.D. Kohler, R. Dieter, N. Meyer and B. Wuerzer, German patent DE 3545904; *Chem. Abstr.*, 107 (1987) P 198109 m.
- [21] S. Iriuchijima, H. Kobayashi, T. Masuda, S. Watanabe and N. Tabata, Japanese patent JP 63267768; *Chem. Abstr.*, 110 (1988) 231620h.
- [22] R. Scholl and G. Mathaiopoulos, *Ber.*, 29 (1896) 1550.
- [23] C.N. Coughlan, H.V. Tartar and E.C. Lingafelter, *J. Am. Chem. Soc.*, 73 (1951) 1180.
- [24] S.E. Hull, D. Viterbo, M.M. Woolfson and Z. Shao-Hui, *MAGEX: a system of computer programs for the automatic solution of crystal structure from X-ray diffraction data*, University of York, UK, 1981.
- [25] G.M. Sheldrick, *SHELX 76: a program for crystal structure determination*, University of Cambridge, UK, 1976.
- [26] Y. Hase, Japan Chemistry Program Exchange, Program No. 035, Updated Version 3.1, 1993.
- [27] U. Burkert and N.L. Allinger, *Molecular Mechanics*, ACS Monograph 177. American Chemical Society, Washington, DC, 1993.
- N.L. Allinger, *J. Am. Chem. Soc.*, 99 (1977) 8127; MM2 1991 parameters from N.L. Allinger.
- [28] D.M. Schnur and D.R. Dalton, *J. Org. Chem.*, 53 (1988) 3313.
- [29] A. Behrens, W.A.P. Luck and B. Mann, *Ber. Bunsenges. Phys. Chem.*, 82 (1978) 47, and references cited therein.
- [30] G. Geiseller, S. Luck and J. Fruwert, *Spectrochim. Acta; Part A*, 31 (1975) 789.
- [31] S.C. White and H.W. Thompson, *Proc. R. Soc. London Ser. A*, 291 (1966) 460.
- [32] K.F. Purcell and R.S. Drago, *J. Am. Chem. Soc.*, 88 (1966) 919.
- [33] F. Fabian, M. Legrand and P. Poirier, *Bull. Soc. Chim. Fr.*, (1956) 1499.
- [34] R.J. Abraham, J. Fischer and P. Loftus, *Introduction to NMR Spectroscopy*, Wiley, New York, 1988.
- [35] G.C. Levy and G.L. Nelson, *J. Am. Chem. Soc.*, 94 (1972) 4897.
- [36] F. Bordwell and G.-Z. Ji, *J. Org. Chem.*, 57 (1992) 3019.
- [37] R. Rittner, *Quim. Nova*, 8 (1988) 170.
- [38] R. Rittner, J.A. Vanin and B. Wladislaw, *Magn. Reson. Chem.*, 26 (1988) 51.
- [39] H. Duddeck and H.T. Feuerhelm, *Tetrahedron*, 36 (1980) 3009.
- [40] A.N. Nesmeyanov, V.A. Blinova, É.I. Fedin, I.I. Kritskaya and L.A. Fedorov, *Dokl. Chem. (Engl. Transl.)*, 220 (1975) 162.
- [41] J.B. Meeks, H.J. Maria, P. Print and S.P. McGlynn, *Chem. Rev.*, 75 (1975) 603.
- [42] M.J.S. Dewar, *Hyperconjugation*, Ronald Press, New York, 1962.
- [43] H. Schmidt and A. Schweig, *Angew. Chem., Int. Ed. Engl.*, 12 (1973) 307.
- [44] H. Ozata, H. Onizaka, Y. Nikey and H. Yamada, *Bull. Chem. Soc. Jpn.*, 46 (1973) 3036.
- [45] K. Kimura and K. Osafune, *Mol. Phys.*, 29 (1975) 1073.
- [46] A. Modelli, G. Distefano and D. Jones, *Chem. Phys.*, 73 (1982) 395.
- [47] G. Distefano, personal communication, 1994.
- [48] A. Modelli, F. Scagnolari, G. Distefano, D. Jones and M. Guerra, *J. Chem. Phys.*, 96 (1992) 2061.
- [49] M. Guerra, D. Jones, G. Distefano, F. Scagnolari and A. Modelli, *J. Chem. Phys.*, 94 (1991) 484.
- [50] R. Fruttero, R. Calvino, B. Ferrarotti, A. Gasco and P. Sabatino, *J. Chem. Soc. Perkin Trans., 2* (1992) 121.
- [51] G.A. Jeffrey, J.R. Ruble and J.A. Pople, *Acta Crystallogr., Sect. B*, 38 (1982) 1975.
- [52] G.A. Jeffrey, J.R. Ruble, R.K. McMullan, D.J. DeFrees and J.A. Pople, *Acta Crystallogr., Sect. B*, 37 (1981) 1381.
- [53] J.C. Giordan, H. Moore, J.A. Tossell and W. Kaim, *J. Am. Chem. Soc.*, 107 (1985) 5600.
- [54] A. Modelli, D. Jones, G. Distefano and M. Tronc, *Chem. Phys. Lett.*, 181 (1991) 361.